объединенный
институт
ядерных
исследований
дубна

E2-88-493 e

B.Z.Kopeliovich, B.G.Zakharov*

NOVEL MECHANISMS OF BARYON NUMBER FLOW OVER LARGE RAPIDITY GAP

Submitted to Zeitschrift für Physik C: Particles and Fields

* Institute of Earth Physics, The USSR Academy of Sciences, Moscow

1988

1. Introduction

Experimental data on soft hadronic processes are described well in the framework of the quark-gluon string model (QGSM)[1-7]. The basis of QGSM is the topological expansion (TE)[8,9] which corresponds in QCD to the 1/N expansion ($N=N_c$, N_c/N_f=const)[10]. The space-time picture of particle production, corresponding to the cut of each sheet, is assumed in QGSM to be connected with decay of chromoelectric tube (string)[11-13].

Unfortunately, theoretical foundation of TE in QCD exists only for meson-meson interaction. The equality of N_c to the number of quarks in a baryon does not allow to use 1/N expansion in the reactions with baryon participation.[14,15]. The quark pair in the colour anti-triplet state (called diquark,D) is similar to anti-quark. Thus, baryon is considered in QGSM as the diquark-quark meson. However, the rigour of this prescription is very questionable, since there are no prohibition for conversion of the diquark into colour sexstet state i.e. the diquark destruction. The universality of the baryon and meson Regge-trajectory slopes[16] and considerations on the minimal energy string configuration for baryon give some arguments in favour of a baryon being a two-body q-D system. However, this concerns the structure of the nucleon wave function (WF), rather than the concept of diquark as an entity participating in the hadronic reactions.

The processes accompanied by the diquark destruction are beyond the QGSM. The examples are the $\bar{N}N$ annihilation or the baryon number flow over large rapidity gap. Indeed, both the diquark momentum distribution F(x) in the WF of the incident baryon and the function of diquark fragmentation into baryon D(z) (we mean "valence" baryon) decrease steeply as the momentum fractions x or z respectively tend to zero. Thus, if the diquark is not destroyed it produces the baryon in the projectile fragmentation region. Hence, the only way to throw a baryon far away from the fragmentation region (of course, excluding sea $\bar{N}N$ pairs), or to cause annihilation in the high energy $\bar{N}N$ interaction, is to form such a colour string configuration, where diquark cannot be treated as an indivisible object.

In view of troubles with straightforward generalization of the 1/N expansion to the baryonic reactions, Rossi and Veneziano[14,15] suggested to classify diagrams according to their topological properties. The crucial point of their approach was a concept of the colour string junction (SJ). From the point of view of TE, the space-time pattern of SJ corresponds to the interception of three sheets. In the string model[19], where a baryon has a form of Y, SJ is a point, where three strings are coupled.

The asymptotics of high energy $\bar{N}N$ annihilation in this approach[14,15] is connected with $\overline{SJ}$-SJ annihilation. Correspondingly, the baryon number can be thrown over a large rapidity gap by means of the SJ transmission[20]. From this point of view, SJ is a part of the diquark, which is destroyed, if SJ is removed.

A consistent quantitative approach to the above described processes is as yet lacking.For this reason, it is worthy to use the methods of the QCD perturbation theory. Strictly spiking, in soft processes one uses perturbative QCD beyond the region of its applicability. Yet, remarcably, it successfully reproduces the most important qualitative and quantitative features of soft hadronic interactions: weak energy dependence of σ_{tot}, small value of ratio σ_{el}/σ_{tot}, strong correlation of σ_{tot} with the hadronic size, etc.[11,21,22]. Of course, perturbative QCD can be used only for the estimation of the definite string configuration production cross section. The decay of the strings is essentially a nonperturbative process, which can be described by a phenomenological approach. It is generally assumed that the history of creation of a string does not influence its decay. This assumption is justified by the agreement with the experimental data of the s-channel factorization relations [23] for the Regge trajectories.

Mechanisms of $\bar{N}N$ annihilation along this approach were considered in papers[24-26]. It was found that asymptotic contribution to the annihilation [24] is described in the Born approximation by the two-gluon exchange in the colour decuplet state. The final state $(3q)_{\{10\}}-(3\bar{q})_{\{\overline{10}\}}$ has a topology of three sheets, i. e. corresponds to annihilation channels.This contribution is energy-independent and it has been estimated at about 1 ÷ 2 mb.

This annihilation contribution to the $\bar{p}p$ total cross section is compensated by another mechanism having two-sheet topology. Both contributions correspond to different cuts of the four-gluon diagram with {10}-{$\overline{10}$} colour state in the t-channel, called a decameron. Nevertheless, decameron contribution to the difference of $\bar{p}p$ and pp multiplicity distributions does not vanish. The analysis[26] of corresponding data up to ISR energies has lead to $\sigma_{\{10\}}$=1.5±0.1 mb, in a good agreement with the perturbative estimation.

It is impossible to extract this small constant tail from the existing (up to 12 GeV) data on annihilation cross section, which demonstrate energy-dependence $\propto 1/\sqrt{s}$. The preasymptotic annihilation mechanisms [25] are connected with presence of slowed down valence quarks in the WF of projectile nucleons and that explains the observed energy dependence. The probability of diquark destruction during the interaction was estimated in the one-gluon approximation. From the point of view of unitarity some of the preasymptotic annihilation mechanisms are included to the Pomeron, others can be treated as a nonplanar corrections to the ω-Reggeon.The calculations[25] show that these preasymptotic mechanisms can explain an order of magnitude of the measured annihilation cross section at energies about 10 GeV.

In present paper we consider from the same point of view the ph interaction with proton flow over large rapidity gap to the central region. The corresponding diagram is shown in fig. 1. The

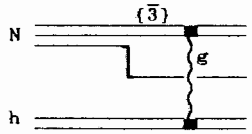

Fig. 1. The lowest order diagram with one-gluon exchange and diquark destruction.

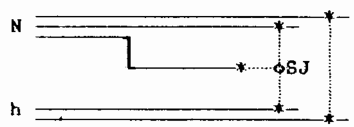

Fig. 2. The final state configuration of colour strings, corresponding to diagram in fig. 1.

proton valence quark is slowed down and is located in the central rapidity region. One-gluon exchange converts the fast colour antitriplet diquark $D_{\{\bar{3}\}}$ into colour sexstet state $D_{\{6\}}$. The nonperturbative stage of final state interaction is connected with formation in the QCD vacuum of the octet colour string (chromo-electric tube) in the rapidity interval between valence quark and hadron h and of sextet colour string in the interval between quark and sextet diquark. In the leading 1/N approximation the hadronization of this system looks the same as in the case of string configuration, shown in fig. 2. The dotted lines in fig. 2 correspond to the colour triplet strings; hadron h is represented here as a system of colour triplet-antitriplet.

Hadronization of string configuration, shown in fig. 2 obviously gives rise to a baryon with the same rapidity as the quark in fig. 1 has. The probability to find a slowed down valence quark in the WF of the incident nucleon is closely related to the growth of inclusive spectra in the central rapidity region with energy[3], so it is fixed by the data.

Thus, the processes with baryon number flow to the central rapidity region give a straightforward information concerning the role of diquark destruction. An analysis of the experimental data[27-29] on the reactions $pp \to p(\bar{p})X$ and $\bar{p}p \to p(\bar{p})X$ in the central rapidity region at ISR energies, carried out below, demonstrates a good agreement with the predictions of the mechanism, shown in figs. 1,2. The contributions other than the diquark destruction are too small to explain the data.

Because of uncertainties in the hadronization of a string configuration with SJ located in the fragmentation region, straightforward calculation of the contribution of the diagrams in fig. 1,2 to the nucleon flow over the whole rapidity interval into the hadron h fragmentation region is not yet possible. One can predict, nevertheless, the energy-dependence $\propto 1/\sqrt{s}$ of this contribution at the fixed value of the Feynmann variable x, what is in agreement with the high-energy data on the processes $\pi^+(\pi^-)p \to p(\bar{p})X$. The impossibility of selfconsistent description of both reactions in the standard version of the QGSM, was emphasized in paper[30].

Present paper is organized as follows. In sect. 2 we estimate the contribution of the mechanism, shown in fig. 1, to the inclusive cross section of the reaction $ph \to pX$ ($h = p,\bar{p}$) in the central rapidity region. The results of the calculations are compared with the experimental data in sect. 3. The considerable probability of the diquark destruction influences some parameters of QGSM. This problem is discussed in sect. 4. In analogy to decameron contribution to the high energy baryon-antibaryon annihilation, baryon number can be transferred by one gluon only. Contribution of gluon mechanism to baryon number flow does not depend on rapidity. It is a subject of sect.5.

In Conclusion we considere some topics for future investigation: i) We propose a new mechanism for baryon-antibaryon pair production which differs principially from Schwinger-like tunnelling from vacuum. This mechanism is characterized by long range rapidity correlations. It is present in hadronic interactions but is absent in e^+e^- collision. ii) A by-product of present consideration is an effective way of spin polarization flow over large rapidity gap. iii) In a proton-heavy nucleus interaction a large portion of incident diquarks, up to 2/3, are destroyed. As the result, the hard part of proton momentum spectra gets poorer. This explains, may be, the observed high value of nuclear stopping power.

2. Formulae for $ph \to pX$ inclusive cross section

The contribution of the diagram of fig. 1 to the inclusive cross section of the reaction $ph \to pX$ in the central rapidity region can be estimated as

$$\frac{d\sigma}{dy}(ph \to pX) \approx K\, \sigma_{\langle 6\rangle} W(y,s). \qquad (1)$$

Here K is the spin-isospin factor; $W(y,s)$ is the nucleon valence quark rapidity distribution in the WF of the incident p-h system. Factor $\sigma_{\langle 6\rangle}$ is the cross section of the process $D_{\langle\bar{3}\rangle}h \to D_{\langle 6\rangle}h_{\langle 8\rangle}$, estimated in the one-gluon exchange approximation (fig. 1). It should be emphasized that notation $\sigma_{\langle 6\rangle}$ stands here for quantity somewhat different from that in paper[25]. Namely, in the case of h=N and nucleon considered as q-D system we imposed in[25] a condition of keeping the diquark in the colour triplet state after interaction. But here we sum over all the possible octet final states of hadron h. Thus we obtain

$$\sigma_{\langle 6\rangle} = \frac{\alpha_s^2}{4}\int \frac{d^2\vec{q}}{\vec{q}^{\,4}} \sum_{\langle 6\rangle,\langle 8\rangle} \langle D_{\langle\bar{3}\rangle}|\sum_{i=1}^{2}\hat{\lambda}_i^{\alpha}\exp(i\vec{q}\vec{r}_i)|D_{\langle 6\rangle}\rangle \,*$$

$$\langle D_{\langle 6\rangle}|\sum_{j=1}^{2}\hat{\lambda}_j^{\beta}\exp(-i\vec{q}\vec{r}_j)|D_{\langle\bar{3}\rangle}\rangle\ \langle h|\sum_{k=1}^{n_h}\tilde{\lambda}_k^{\alpha}\exp(-i\vec{q}\vec{r}_k)|h_{\langle 8\rangle}\rangle \,*$$

$$\langle h_{\langle 8\rangle}|\sum_{l=1}^{n_h}\tilde{\lambda}_l^{\beta}\exp(i\vec{q}\vec{r}_l)|h\rangle . \qquad (2)$$

Here α_s is the QCD coupling constant; $\tilde{\lambda}^{\alpha} = \hat{\lambda}^{\alpha}((\hat{\lambda}^{\alpha})^T)$ for quarks (anti-quarks); n_h is the number of quarks or anti-quarks in hadron h.

The summing over $D_{\langle 6\rangle}$, i.e. space and spin-isospin parts of the sextet diquark WF can be carried out without restrictions imposed by the Pauli principle. The sum over colour part of the sextet diquark WF is equal to (i,j,k,l are the quark colour indices)

$$\sum_{\langle 6\rangle} \langle i,j|\{6\}\rangle \langle\{6\}|k,l\rangle = \frac{1}{2}\,(\delta^i_k\,\delta^j_l + \delta^i_l\,\delta^j_k). \tag{3}$$

Using this formula together with relation

$$\langle i,j|\{3\}_k\rangle = \frac{1}{\sqrt{2}}\,\varepsilon_{ijk}$$

and summing over WF of the hadron h in the octet colour state, we obtain

$$\sigma_{\langle 6\rangle} = \frac{4\pi}{3}\,\alpha_s^2\,n_h \int_0^\infty \frac{d^2\vec q}{\vec q^{\,4}}\,\left[1-F_D(\vec q^{\,2})\right]\,\left[1-F_h(\vec q^{\,2})\right]. \tag{4}$$

Here

$$F_i(\vec q^{\,2}) = \langle i|\exp\left[i\vec q(\vec r_k-\vec r_l)\right]|i\rangle;$$

(i=D,h) are the double-quark form factors of diquark and hadron h.

Note, that expression (4) is infra-red convergent. That is a consequence of hadron h being colourless and the fact that the long-wave gluon cannot resolve the inner structure of the compact diquark.

Let us use the nonrelativistic oscillator functions to calculate the form factors $F_i(q^2)$.

$$F_i(\vec q^{\,2}) = \exp(-\alpha_i q^2), \qquad i=D,h, \tag{5}$$

$$\alpha_D = 2/3r_D^2\,,$$

$$\alpha_h = \begin{cases} r_p^2/2\,, & \text{if } h = p,\bar p \\ 2r_\pi^2/3, & \text{if } h = \pi \end{cases}$$

Here r_D^2 is the mean diquark radius squared; $r_p(r_\pi)$ is a mean charge proton (pion) radius. The proton form factor $F_2(\vec q^{\,2})$ is practically independent on the diquark radius if r_p is fixed.

Now, expression (4) is easily transformed to

$$\sigma_{\langle 6\rangle} = \frac{4\pi}{3}\,\alpha_s^2\,n_h\,J(\alpha_D,\alpha_h) \tag{6}$$

$$J(a,b) = a\,\ln\left(\frac{a+b}{a}\right) + b\,\ln\left(\frac{a+b}{b}\right).$$

Constant α_s is determined from the cross section of process $hN \to h_{\langle 8\rangle}N_{\langle 8\rangle}$ calculated in the one-gluon exchange approximation

$$\sigma(hN \to h_{\langle 8\rangle}N_{\langle 8\rangle}) = \frac{8\pi}{3}\,\alpha_s^2\,n_h J(\alpha_p,\alpha_h). \tag{7}$$

This expression should be normalized to a difference $\sigma^{hN}_{tot} - \sigma^{hN}_{el} - \sigma^{hN}_{DD}$ rather than σ_{tot}, because the cut of the two-gluon graph does not contain colourless two-particle intermediate state.

Now, there is ample evidence that the compact diquark component of the nucleon WF is dynamically enhanced for some reasons. That are the deep inelastic lepton scattering data analysis [31-34], processes with large p_T proton production [35-38], calculations in the instanton vacuum model [39] lastly. Thus, we are enforced to consider two types of the nucleon WF: i) the symmetrical oscillator WF for which $r_D = \sqrt{3}/2\ r_p \approx 0.7$ F (variant I); ii) we add the 50% admixture of compact diquark of radius $r_D = 0.4$ F (variant II).

The numerical calculations in (6) for these two variants lead to

$$\sigma_{\langle 6\rangle}(h = \bar p, p) = \begin{cases} 15\ \text{mb} & (I) \\ 11\ \text{mb} & (II). \end{cases} \tag{8}$$

We fixed $\sigma(pp \to p_{\langle 8\rangle}p_{\langle 8\rangle}) = 30$ mb. To relate cross sections of different processes we have taken the running QCD coupling constant $\alpha_s(q^2)$ in the one-loop approximation. If $r_D = 0.4$ F, the value of α_s is 15% smaller than that deduced from Eq.(7).

Let us estimate now the function W(y,s) in expression (1). We use the following parameterization [4,40] for the momentum distribution of quarks in the proton

$$q(x) = C_1 x^{-\alpha_R(0)}\,(1-x)^{\beta-1}, \tag{9}$$

where x is a fraction of proton momentum carried by a quark;

$$\beta = \alpha_R(0) - 2\alpha_N(0) - 1;$$

$$\alpha_R(0) = 0.5; \quad \alpha_N(0) = -0.5;$$

$$C_1 = \frac{\Gamma(1-\alpha_R(0)+\beta)}{\Gamma(\beta)\Gamma(1-\alpha_R(0))} \approx 0.85.$$

Then the probability of string configuration in fig. 2 with valence quark having rapidity y (in c.m. frame) is found to be

$$W(y,s) \approx C_1\left(\frac{m^T_q}{\sqrt{s}}\,e^y\right)^{1-\alpha_R(0)}, \tag{10}$$

where $m^T_q = \left(m^2 + \langle (p^T_q)^2\rangle\right)^{1/2}$.

Strictly speaking, one should take into account the possibility of formation of supplementary $\bar q q$-strings, coupled to the sea $\bar{q}q$ pairs in the projectile nucleon WF. This is achieved by means of substitution of factor C_1 by C_{eff}, where

$$C_{eff} = \sum_{n=1}^{\infty} C_n \frac{\sigma^n_{in}}{\sigma_{in}} . \qquad (11)$$

Here σ^n_{in} is a contribution to σ_{in} connected with the cut of n Pomerons[41]; C_n is a normalization factor in the formula for x-distribution of quark at $x \to 0$ in the case of existence of n-1 supplementary sea $\bar{q}q$ pairs. This formula is obtained[40] by means of change $\beta \to \beta$-n+1 in formula (9). At ISR energies where some data exist now, the quasi-eikonal model for σ^n_{in} leads to estimation $C_{eff} \approx 1$.

We evaluated $m^T_q \approx 0.4$ GeV in formula (10) putting $m_q \approx 0.3$ GeV, $\langle (p^T_q)^2 \rangle \approx 0.15$ (GeV/c)^2.

It should be emphasized that expression (10) for W(y,s) (with substitution $C_1 \to C_{eff}$) seems to be highly reliable, because it also determines the growth of the inclusive cross section with energy in the central rapidity region. This growth is connected in QGSM[9] with large contribution of the topological diagram with underdeveloped cylinder and is sensitive to a probability to find a valence quark in the central region. Function W(y,s) in form (10) with $m^T_q = 0.4$ GeV and $C_{eff} = 1$ describes well the growth of the inclusive spectra at y=0 in the energy intervals of ISR and ISR - $Sp\bar{p}S$ collider. Thus, W(y,s) can be considered as determined directly from the experiment.

We conclude with the estimation of spin-isospin factor K in (1). Let us make some simplifying assumptions: i) only the N and Δ are produced in the central region; ii) production of s-quark is suppressed by factor 1/3; iii) the relative probabilities of u and d quark flows are equal to 2:1. Then factor K is estimated as $K \approx 0.5$.

Finally, the cross section of the proton flow to the central rapidity region p+p($\bar{p}$) → p+X estimated by using expressions (1), (8) and (10), is equal to

$$\frac{d\sigma}{dy}(ph \to pX) \approx \left(\frac{1\ \text{GeV}}{\sqrt{s}}\right)^{1-\alpha_R(0)} \Big\{ \exp\left(y\left[1-\alpha_R(0)\right]\right) +$$

$$\varepsilon \exp\left(-y\left[1-\alpha_R(0)\right]\right)\Big\} * \begin{cases} 4.7\ \text{mb}, & (I) \\ 3.5\ \text{mb}, & (II) \end{cases} , \qquad (12)$$

where

$$\varepsilon = \begin{cases} 0, & \text{if } h = \bar{p} \\ 1, & \text{if } h = p . \end{cases}$$

The cross section of the process $p+\bar{p} \to \bar{p}+X$ is obtained from (12) by means of substitution $y \to -y$ (proton momentum corresponds to positive y).

3. Comparison with the experimental data

To determine the cross section of proton flow to the central rapidity region one should consider the difference $\Delta d\sigma/dy = d\sigma(pp\to pX)/dy - d\sigma(pp\to \bar{p}X)/dy$ in order to remove the sea $\bar{N}N$ pairs. The experimental points shown in fig. 3 in the energy interval $\sqrt{s}$ = 23 ÷ 63 GeV have been obtained by means of integration of the data[27] parameterized as A exp(− Bp_T) with parameters fitted in[27]. Another parameterization in the form A exp(-Bp_T- Cp_T^2), which has also been used in[27], results in the close (within about 10%) values of the cross section.

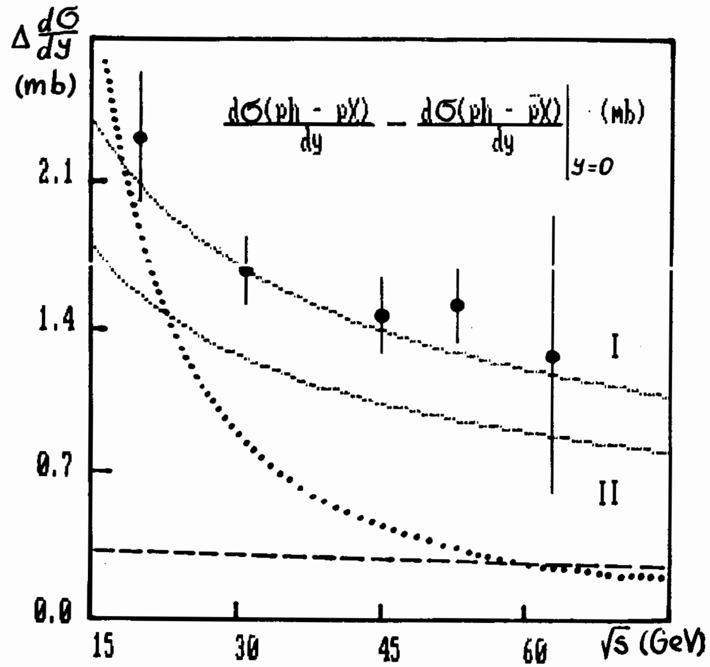

Fig.3. Difference of p and $\bar{p}$ production cross sections at y=0 in pp collision at ISR[27]. Curves I and II correspond to expression (12). Dotted line shows the contribution of diquark fragmentation[40] into proton. Dashed line indicates the contribution connected with the difference of quark fragmentation probabilities into p and $\bar{p}$.

The fit of the data in fig. 3 by the function $\Delta d\sigma/dy=b(\sqrt{s})^{-\beta}$ yield parameters $b=8.7\pm6.4$, $\beta=0.46\pm0.21$, which are in excellent agreement with estimation (12). Two corresponding curves plotted in fig. 3 characterize the theoretical uncertainty.

The rapidity-dependence of the inclusive cross sections has been measured in [28] in the interval $-0.4 \le y \le 0.4$. The results are presented in the form of ratios

$$R_{p(\bar{p})} = \frac{d\sigma[\,p\bar{p}\to p(\bar{p})X]/dy}{d\sigma[\,pp\to p(\bar{p})X]/dy}. \qquad (13)$$

In order to test prediction (12) for the y-dependence of baryon number flow let us parameterize $R_{p(\bar{p})}$ in the following form (the projectile proton has positive rapidity):

$$\frac{d\sigma}{dy}(p\bar{p}\to\bar{p}X) = \delta\alpha + \beta e^{-\tau y}$$

$$\frac{d\sigma}{dy}(pp\to\bar{p}X) = \alpha$$

$$\frac{d\sigma}{dy}(p\bar{p}\to pX) = \delta\alpha + \beta e^{\tau y} \qquad (14)$$

$$\frac{d\sigma}{dy}(pp\to pX) = \alpha + \beta(e^{\tau y}+e^{-\tau y}).$$

The first terms here result from the $\bar{N}N$ pair production from the vacuum. Other terms include the contribution of baryon flow to the central rapidity region. The factor δ takes into account the small difference between the charged particle inclusive spectra in pp and $\bar{p}p$ collisions and is close to unity.

The fit of the experimental data[28] shown in fig. 4 by formulae (14) gives

$$\tau = 0.76 \pm 0.22$$
$$\delta = 1.01 \pm 0.02 \qquad (15)$$
$$\beta/\alpha = 0.3 \pm 0.03.$$

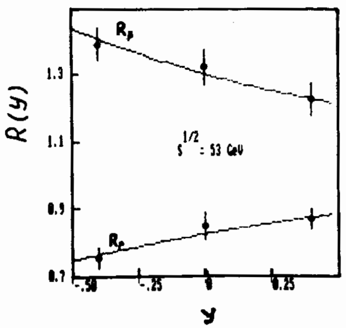

Fig. 4. Data[28] on the ratio $R_{p(\bar{p})}(y)$ defined in (13). The curves are the results of the fit by means of expressions (14) with parameters (15).

The found value of τ is consistent within the error bars with the predicted one (12). The ratio of charged particle spectra in $\bar{p}p$ and pp interactions[20] is also consistent with the value of δ.

The value of parameter α in (14) is known from the data[28]: $d\sigma/dy(pp\to\bar{p}X) = 1.7 \pm 0.1$ mb at $\sqrt{s} = 53$ GeV. Thus, one can determine the parameter $\alpha=0.51 \pm 0.06$, which is also in agreement with estimation (12). Thus, both the sets[27,28] of data agree well with the considered model of the proton flow over large rapidity gaps.

Note, that it is hard to explain in another way the observed[27,28] high yield of protons in central rapidity region. This ISR data cannot be understood in the frame work of QGSM with indivisible diquark. Calculation of the baryon spectrum has been performed in such approach in papers [40]. Though the central region $y \approx 0$ has not been considered there, the diquark fragmentation function $D^p_D(z)$ used in[40] gives too steep decrease of the baryon spectrum with the energy: $d\sigma/dy|_{y=0} \propto s^{-1}$ (we mean the valence protons).

It is interesting that there exists some additional contribution to the difference of $\bar{p}$ and p spectra $\Delta d\sigma/dy$ in QGSM which decreases with energy as $s^{-1/4}$, i.e. in the same way as is predicted by (12). Nevertheless, it is not connected with diquark destruction. Indeed, the quark fragmentation functions $D_q^{p(\bar{p})}(z)$ are different for p and $\bar{p}$. Thus, in the case, when one of the projectile valence quarks has $x \approx 0$, the probabilities to find a sea p or $\bar{p}$ in neighbourhood of quark in the rapidity scale are slightly different, even if diquark is not destroyed. In another words, one can say that existence of projectile quark in the central region distorts the sea.

Both contributions are plotted in fig. 3. We can see that one of them too steeply decreases with energy, but another one is negligibly small. We omit here the details of the calculation which are well described in [40]. Few comments should be made, nevertheless.

- We use slightly different value of parameter a_p, which controls the $\bar{N}N$ pair production in the colour triplet string hadronization. Instead of the value $a_p = 0.07$ used in [40], we fix $a_p = 0.055$ from the data[28] on $d\sigma(pp\to\bar{p}X)/dy$. This value agrees well with the results of paper [30].
- In the reaction $pp\to pX$ both protons contribute to the central region, so the results of calculations[40] at $\sqrt{s} = 20$ GeV should be doubled because the fragmentation of only one of the projectile protons has been taken into account there.

Another evidence in favour of considered mechanism comes from an analysis of the data on difference between the cross section of reactions $\pi^+p \to pX$ and $\pi^-p \to \bar{p}X$ in the pion fragmentation region[42,43]. The observed considerable difference is much larger than predicted by the triple-Regge formalism:

$$\left(\frac{\Delta\, d\sigma/dx}{\Sigma\, d\sigma/dx}\right)_{NN\omega} \approx N\, \sqrt{(1-x)s_0/s}\ , \qquad (16)$$

where $\Delta d\sigma/dx$ and $\Sigma d\sigma/dx$ are the difference and the sum of the $\pi^+ \to p$ and $\pi^- \to p$ inclusive cross sections. Factor $N \approx 1$. Impossibility of joint description of these data in the approach, where $p(\bar{p})$ comes from the pion fragmentation only, was claimed also in paper[30].

Unfortunately, we are unable to calculate accurately a probability of the proton flow to the pion fragmentation region $x \to 1$. The energy dependence at fixed value of x should be $\propto 1/\sqrt{s}$, i.e. the same as is given by relation (16). The fit to the data[42-43] at $x = 0.5$ with power dependence s^{β} gives $\beta = -0.56\pm0.11$.

In the Regge phenomenology one describes the production of particles in the central rapidity region by means of the Mueller[45]- Kancheli[46] diagram, shown in fig. 5. The double Pomeron diagram does not contribute to the baryon - antibaryon cross section difference. The ramaining Regge singularities are the ω- and ρ-poles and those, which contribute to the annihilation cross section. However, their relative residues are quite different and should be deduced from some dynamics model.

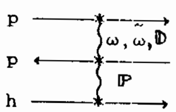

Fig. 5. The Mueller - Kancheli diagram for proton production in the central rapidity region.

The baryon number flow over large rapidity gap was considered also in paper[47] in the frame work of multiperipheral model with baryon exchange. It was prescribed to the inclusive cross section (arbirtrarily to some extent) the same energy-dependence as is observed in the annihilation. The crudely estimated cross section[47] turns to be close (two times larger) to one found here. The authors[47] connected erroneously this mechanism with the ω-IP Mueller - Kancheli diagram. In fact, this diagram corresponds to the case of valence quark flow to the central region without diquark destruction, which was considered above. It contributes to the difference between proton-antiproton production cross sections due to dissimilarity of fragmentation functions $D^{p}_{q}(z)$ and $D^{\bar{p}}_{q}(z)$. The contribution of this mechanism was found to

be negligibly small. Actually, the multiperipheral baryon exchange[47] corresponds to $\tilde{\omega}$ - IP Mueller-Kancheli diagram, where $\tilde{\omega}$ is a nonplanar correction to the ω - Reggeon[25]. This is just the mechanism shown in figs. 1,2 and considered in sect. 2 of present paper.

4. Some consequences for QGSM

Considerable probability of the diquark destruction given by (8) can result in noticeable change of some QGSM parameters.

Determination of the diquark→proton fragmentation function $D^{p}_{D}(z)$ contains some arbitraryness. In the approach[44] which exploits the cascade equations the result depends on choosing of the equation cores. Another approach[4,40] uses some smooth interpolation between the two Regge-asymptotics $z \to 0$ and $z \to 1$. The relation between the momenta of the produced baryons and mesons is not fixed and can be changed not contradicting the baryon number and total momentum conservation sum rules. The main criterion of correctness of the diquark fragmentation functions is a quality of description of the particle momentum spectra in ph collisions. However, the possibility of diquark destruction results in more hard fragmentation functions $D^{p}_{D}(z)$. Indeed, the string configuration in fig. 2 produces during hadronization mainly soft protons with $x \approx 0.5$, because the valence quark carries in average only about 10% of the baryon momentum (including supplementary $\bar{q}q$ sea pairs). On the other hand this mechanism provides considerable contribution to the high momentum part of the pion spectrum. Let us estimate this contribution.

The quark momentum distribution inside a diquark can be parameterized as

$$f_{q/D}(x) = A\, x^{n}(1-x)^{n}. \qquad (17)$$

Use of this expression with n=2.5 and the fragmentation function $D^{\pi}_{q}(z)$ from paper[4] allows to obtain a good description of pion spectra[44]. As the distribution (17) decreases steeply at $x \to 0,1$, the string configuration in fig. 2 cannot produce a proton with $x_F \approx 1$.

Note that the distribution (17) in the region $1-x_F \geq 0.05$ is similar within accuracy of about 20÷30% to that which can be obtained for the relativistic two-body diquark WF

$$\Psi_D(x,p_T) \propto \frac{1}{\sqrt{x(1-x)}}\, \exp\left[-\frac{\alpha(m_q^2+p_T^2)}{x(1-x)}\right]\ . \qquad (18)$$

with parameters $m_q \approx 0.27$ GeV, $\alpha \approx 1.5 \div 2$ GeV^{-2}. Such WF corresponds to the diquark with the radius $r_D \approx 0.4 \div 0.5$ F.

We can conclude now, that the hard part of the baryon spectrum is determined mainly by the mechanisms with indivisible diquarks. At the same time production of high momentum pions results mainly from diquark destruction. Naturally, the situation becomes reversed when one considers the soft part of the spectra (in the c.m. frame).

5. Gluon mechanism of baryon number flow.

As was mentioned in the Introduction, the behaviour of the annihilation cross section at asymptotic energies is governed by the decameron exchange, introduced in papers[24,26]. An analysis of the experimental data on the difference between $\bar{p}p$-pp multiplicity distributions demonstrates that decameron contribution is energy-independent up to ISR energies $\sqrt{s} \approx$ 50GeV. This fact and the cross section value justifies the calculations[24] in the perturbative QCD.

It is natural to believe that there exists decameron contribution to the Mueller-Kancheli diagram shown in fig. 5. The corresponding inclusive cross section is energy- and rapidity-independent. Unfortunately, it is hard to propose any rigorous calculation of the cross section value. We give here a crude estimation only.

Let us considere the lowest order perturbative graph shown in fig. 6, which corresponds to the cut of the Mueller-Kancheli diagram of fig. 5 with $\mathbb{P}$-$\mathbb{P}$ exchange. The corresponding string configuration shown in fig. 7 demonstrates, indeed, that baryon is

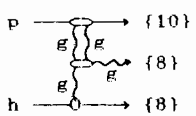

Fig.6. Perturbative QCD graph with transformation of the projectile 3-quark system into colour decuplet state.

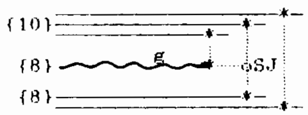

Fig.7. Final state string configuration corresponding to the graph in fig. 6.

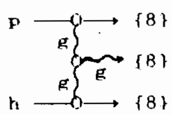

Fig.8. Mueller-Kancheli diagram corresponding to figs. 6, 7.

produced with the same rapidity as gluon has. To estimate the fig.6 cross section we suppose that it is suppressed in comparison with contribution of graph in fig.8 in the same manner as the cut of decameron in comparison with Pomeron, i.e. by a factor about 1/20. Some justification of this assumption comes from the fact that upper blocks are the same in both cases. Moreover, any number of gluons with rapidities smaller than the produced baryon has, are allowed to be emitted in figs.6,8. On the other hand, the graph in fig.8 corresponds to the higher order corrections of ladder type to the two-gluon contribution to the Pomeron. These corrections are responsible for the Pomeron Reggeization and can be evaluated from phenomenology. QCD motivated[48,49] analysis[50] of the experimental data found that the contribution of this perturbative corrections to the pp total cross section is about 10 mb at ISR energies. Finally, one should take into account the spin-isospin factor of about 0.5 for proton production. Gathering all the factors together we obtain an estimate $d\sigma(pp \to pX)/dy \approx 0.1$ mb for the contribution of graph of fig.6. Comparison with the experimental data in fig.3 shows that the relative decameron contribution is small till the ISR energies, but it becomes considerable at S$\bar{p}$pS collider and future accelerator energies.

6. Conclusion

The process of baryon number flow over large rapidity gap is bejond the QGSM as it is accompanied by diquark desintegration. From the point of view of the Mueller-Kancheli diagram it is goverened by the same mechanisms as the antiproton-proton annihilation is. But if an experimental investigation of the latter process is practically impossible at high energies, the former is highly suitable, particularly for collider mashines.

We ascertained here two new mechanisms for the incident baryon number transfer to the central rapidity region at high energies. One is connected with possibility to find a slow valence quark in the WF of high energy proton and with destruction of a diquark-spectator by means of converting it into the sextet colour state. In another words, the valence quark is a carrier of baryon number in this case (from the point of view of topological expansion the quark is excorted by SJ). The most intriguing possibility is the second one: the carrier of baryon number in this case is a gluon (SJ in the topological classification).

Let us consider now a few consequeces.

1. There exists a new mechanism of baryon-antibaryon pair production from vacuum, different from the well-known Schwinger one. It is clear that the perturbative Pomeron[48] contains a decameron impurity among the ladder-type graphs. An example is shown in fig.9. Inelastic process corresponding to the cut of this graph is a result of hadronization of string configuration shown in fig.10. As the SJ-$\overline{SJ}$ pair emerged, the baryon-antibaryon pair should be produced with the same rapidities after hadronization. The probability of such configurations is suppressed by an order in comparison with production of "ordinary" colour triplet strings, decaing mainly into $\bar{q}q$ pairs. Thus, the

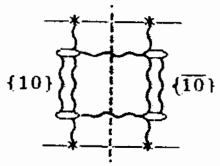

Fig.9. Decameron impurity in the perturbative Pomeron. Dashed line denotes the cut.

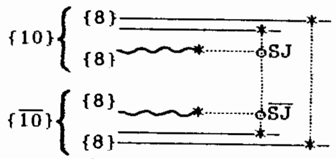

Fig.10. Example of the final state string configuration corresponding to the graph in fig.9.

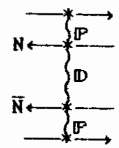

Fig.11. Mueller - Kancheli diagram corresponding to figs. 9,10.

yield of $\bar{N}N$ pairs produced by this mechanism is of the same order as that from Schwinger-like tunnelling from vacuum. They can be distinguished due to long range rapidity correlation inherent in present mechanism.

It is interesting, that such mechanism is absent in e^+e^- collisions. Thus, it explains naturally the observed enlarged relative density of $\bar{N}N$ pairs in the rapidity scale in hadronic interactions at $\sqrt{s}$=540GeV in comparison with e^+e^- collisions.

2. As avalence quark plays a role of the baryon number carrier, it can transfer the incident baryon polarization over large rapidity gap, i.e. in the reaction $h+p^\uparrow \to p^\uparrow + X$ (arrow denotes the polarized protons). If the proton is mainly a system q-D, where D has S=T=0, then the valence quark in the central region in fig.1,2 carries all the incident proton polarization. This mechanism of polarization transmission is dominant at large rapidity intervals. The diminution of polarization due to sea $\bar{N}N$ pairs contribution, resonance production ets. should be taken into account.

3. Destruction of incident diquark during proton-nucleus interaction proceeds with a high probability. Indeed, if the nucleus is heavy enough, fast diquark undergos many colour exchange scatterings (via one-gluon exchange, for instance). As a result, both quarks turn into totally unpolarized state in the colour space. Thus, the quark-pair finds itself with probability 1/3 in the antitriplet colour state (diquark) or with probability 2/3 in the sextet colour state. Corresponding probabilities for real nuclei can be found in[51]. In the latter case the SJ, i.e. nucleon, is formated in the central rapidity region or in the nucleus fragmentation region yet, as it follows from the previous considerations. This phenomenon should considerably influence the momentum spectra of protons in the reaction pA→pX which is intensively discussed in respect with the problem of the so called nuclear stopping power[52-56].

References

1. Cohen-Tannoudji G., Hassouni A.E., Kalinowski J., Peschanski R. Phys.Rev., 1979, D19, p.3397.
2. Kaidalov A.B. Sov. Phys. JETP Lett., 1980, 32, p. 494.
3. Kaidalov A.B. Phys.Lett., 1982, 116B, p. 459.
4. Kaidalov A.B. In: "Elementary Particles", ITEP X School of Physics, M., Energoatomizdat, 1983
5. Capella A., Tran Thanh Van J. Phys.Lett., 1982, 114B, p.450
6. Kaidalov A.B., Ter-Martirosyan K.A. Yad.Fiz., 1984, 39, p.1545.
7. Kaidalov A.B., Ter-Martirosyan K.A. Yad.fiz., 1984, 40,p.211.
8. Veneziano G. Phys.Lett., 1974, 52B, p. 220.
9. Chew V.P., Rosenzweig C. Phys.Rep., 1978, 41, p. 264.
10. Veneziano GV. Nucl.Phys., 1976, B117, p. 519.
11. Low F.E. Phys.Rev., 1975, D12, p. 163.
12. Casher A., Neubergver H., Nussinov S. Phys.Rev., 1979, D20, p. 179.
13. Gurvich E.G. Phys.Lett., 1979, 87B, 386.
14. Rossi G.C., Veneziano G. Nucl.Phys., 1977, B123, p.507.
15. Rossi G.C., Veneziano G. Phys.Rep., 1980, 63, p.149.
16. Migdal A.B. Sov. Phys. JETP Lett., 1987, 46, p.256.
17. Abramovsky V.I., Gribov V.N., Kancheli O.V. Yad. Fiz., 1973,18,p.595
18. Kaidalov A.B. Yad.Fiz., 1987, 45, p. 1452.
19. Artry V. Nucl.Phys., 1975, B85, p. 442.

20. Volkovitsky P.E. Yad. Fiz., 1986, 46, p.268
21. Gunion J.F., Soper D.E. Phys.Rev., 1977, D15, p. 2617.
22. Levin E.M., Ryskin M.G. Yad.Fiz., 1981, 34, p. 1441;
23. Kaidalov A.B. Z.Phys.C, 1982, 12, p.63.
24. Kopeliovich B.Z., Zakharov B.G. JINR, E2-87-548, Dubna, 1987.
25. Kopeliovich B.Z., Zakharov B.G. JINR, E2-88-85,Dubna, 1988.
26. Kopeliovich B.Z., Zakharov B.G. JINR, E2-87-911, Dubna, 1987
27. Alper B. et al. Nucl.Phys., 1975, B100, p. 237.
28. Akesson T. et al. Nucl.Phys., 1983, B228, p. 409.
29. Camilleri L. Phys.Rep., 1987, 53, p. 144.
30. Shabelsky Yu.M. Yad.Fiz., 1986, p. 186.
31. Abbot L.F., Berger E.L., Blakenbecler R., Kane G.L. Phys.Lett., 1979, 88B, p. 157.
32. Fredriksson S. et al. Z.Phys.C, 1982, 14, p. 35.
33. Fredriksson S. et al. Z.Phys.C, 1983, 19, p. 53.
34. Fredriksson S., Larsson T.I. Phys.Rev., 1983, D28, p. 255.
35. Laperashvili L.V. Yad.Fiz., 1982, 35, p. 742
36. Breakstone A. et al. Z.Phys.C, 1985, 28, p.235.
37. Kim V.T. JINR, E2-87-75, Dubna, 1987.
38. Efremov A.V., Kim V.T. JINR, E2-87-74, Dubna, 1987.
39. Betman R.G., Laperashvili L.V. Yad. Fiz., 1985, 41, p. 463
40. Kaidalov A.B., Piskunova O.I. Z.Phys.C, 1986, 30, p.145.
41. Ter-Martyrosyan K.A. Phys.Lett., 1973, 44B, p. 377.
42. Brenner A.E. et al. Phys.Rev., 1982, D26, 1497.
43. Abreu M.G. et al.Z.Phys.C, 1984, 25, p.115.
44. Kinoshita K., Noda H., Tashiro T. Progr.of Theor.Phys., 1982, 68, p. 2086.
45. Mueller A.H. Phys. Rev., 1970, D2, p. 2963
46. Kancheli O.V. JETP Lett., 1970, 11, p. 397
47. Gendenshtein L.E., Kaidalov A.B. Yad.Fiz., 1972, 16, p.1307; JETP Lett., 1972, 16, p. 249.
48. Kuraev E.A., Lipatov L.N., Fadin V.S. Sov. Phys. JETP, 1976, 44, p.443; ibid. 1977, 45, p.199
49. Lipatov L.N. Sov. Phys. JETP, 1986, 63, p.904
50. Kopeliovich B.Z., Nikolaev N.N., Potashnikova I.K. JINR preprints: E2-86-125, Dubna,1986; E2-87-918, Dubna,1987
51. Kopeliovich B.Z., Lapidus L.I. "Colour exchanges of high energy hadrons in nuclei", Proceedengs of the 6-th Balaton Conference on Nuclear Physics, Balatonfüred, Hungary, 1983, p.73

52. Busza W. Lect. Not. Phys., 1985, 221, p. 77
53. Busza W., Goldhaber A.S. Phys. Lett., 1984, 139, p.235
54. Bowling G. Goldhaber A.S. Phys. Rev., 1986, D34, p.778
55. Date S. et al. Phys. Rev., 1985, D32, p.619
56. Gyulasy M. Z. Phys., 1988, C 38, p.361

Received by Publishing Department
on July 6, 1988.

SUBJECT CATEGORIES OF THE JINR PUBLICATIONS

Index	Subject
1.	High energy experimental physics
2.	High energy theoretical physics
3.	Low energy experimental physics
4.	Low energy theoretical physics
5.	Mathematics
6.	Nuclear spectroscopy and radiochemistry
7.	Heavy ion physics
8.	Cryogenics
9.	Accelerators
10.	Automatization of data processing
11.	Computing mathematics and technique
12.	Chemistry
13.	Experimental techniques and methods
14.	Solid state physics. Liquids
15.	Experimental physics of nuclear reactions at low energies
16.	Health physics. Shieldings
17.	Theory of condenced matter
18.	Applied researches
19.	Biophysics

Копелиович Б.З., Захаров В.Г. E2-88-493

Новые механизмы заброса барионного числа через большой интервал быстроты

Показано, что медленный валентный кварк в волновой функции налетающего протона высокой энергии может образовать барион, если дикварк-спектатор расщепился, т.е. перешел в сикстетное по цвету состояние. Мы оценили сечение заброса барионного числа в центральную область быстрот, пользуясь методами теории возмущений КХД. Сечение зависит от интервала быстроты Δy как $\exp(-\Delta y/2)$ и хорошо согласуется с экспериментальными данными при энергии ISR. Существует также интересная возможность передачи барионного числа одним глюоном. Этот вклад не зависит от энергии и быстроты и становится заметным при энергии УНК. Предлагаются также новые механизмы для рождения барион-антибарионных пар из вакуума, передачи поляризации через большой интервал быстроты, тормозящей способности ядер.

Работа выполнена в Лаборатории ядерных проблем ОИЯИ.

Препринт Объединенного института ядерных исследований. Дубна 1988

Kopeliovich B.Z., Zakharov B.G. E2-88-493

Novel Mechanisms of Baryon Number Flow Over Large Rapidity Gap

It is shown that slow valence quark in the wave function of high energy proton can fragment into a baryon if the fast diquark-spectator is destroyed, i.e. is turned from the antitriplet to the sextet colour state. We estimated the cross section of the baryon number flow to the central rapidity region using the perturbative QCD. It depends on the rapidity gap Δy as $\exp(-\Delta y/2)$ and nicely agrees with the data at ISR energies. There exists also an intriguing possibility of transfering baryon number by means of gluonic exchanges only. This contribution does not depend on rapidity at all and becomes sizable in TeV energy region. We propose also new mechanisms for baryon-antibaryon production from vacuum, transfer of polarization over large rapidity intervals, and nuclear stopping power.

The investigtaion has been performed at the Laboratory of Nuclear Problems, JINR.

Preprint of the Joint Institute for Nuclear Research. Dubna 1988